A comparison of the Richardson extrapolation and the approximation error estimation on the ensemble of numerical solutions

Alekseev A.K.[0000-0001-8317-8688], Bondarev A.E.[0000-0003-3681-5212] and Kuvshinnikov A.E.[0000-0003-1667-6307]

Keldysh Institute of Applied Mathematics RAS, Moscow, Russia
aleksey.k.alekseev@gmail.com, bond@keldysh.ru, kuvsh90@yandex.ru

Abstract. The epistemic uncertainty quantification concerning the estimation of the approximation error using the differences between numerical solutions treated in the Inverse Problem statement is addressed and compared with the Richardson extrapolation. The Inverse Problem is posed in the variational statement with the zero order Tikhonov regularization. The ensemble of numerical results, obtained by the OpenFOAM solvers for the inviscid compressible flow with a shock wave is analyzed. The approximation errors, obtained by the Richardson extrapolation and the Inverse Problem are compared with the exact error, computed as the difference of numerical solutions and the analytical solution. The Inverse problem based approach is demonstrated to be an inexpensive alternative to the Richardson extrapolation.

Keywords: Richardson extrapolation, approximation error, ensemble of numerical solutions, Euler equations, OpenFOAM, Inverse Problem.

1 Introduction

The estimation of the approximation error that is a subject of the epistemic uncertainty quantification is the main element for the verification of numerical calculations. The standards [1,2] recommend the Richardson extrapolation (RE) as one of the main tools for the verification of solutions and codes in the Computational Fluid Dynamics. RE provides the pointwise approximation of the approximation error, unfortunately, at the cost of the extremely high computational burden [3-5]. There exist some computationally inexpensive approaches for the approximation error norm estimation, for example [6]. However, these approaches do not provide the pointwise information on the error. Thus, the need for a computationally inexpensive a posteriori estimation of the point-wise approximation error exists. For this reason we consider herein the computationally inexpensive approach to a posteriori error estimation [7] that is based on the ensemble of numerical solutions obtained by different algorithms. The approximation error is estimated using the differences of solutions at every grid node that are treated by the Inverse Ill-posed Problem (IP) stated in the variational statement with the Tikhonov zero order regularization [8,9]. The results of the numerical tests for

ICCS Camera Ready Version 2021
To cite this paper please use the final published version:
DOI: 10.1007/978-3-030-77980-1_42

compressible Euler equations are provided that demonstrate both the estimated error and the exact error (obtained by a comparison of numerical solution with the exact analytical one). The paper [7] analyzed the pointwise error by comparison with the etalon solutions [10]. In the present paper we compare the error computed by Inverse problem with the exact error (engendered by the analytic solutions) and the results by the Richard-son extrapolation.

2 The Richardson extrapolation for flows with discontinuities

We consider the numerical solution u_h obtained by some CFD solver, the exact (unknown) solution $\tilde{u}$, the approximation error $\Delta u = u_h - \tilde{u}$. The Richardson extrapolation (RE) applies two numerical solutions obtained for consequently refined grids for the pointwise (m is the number of the coarse grid point) estimation of exact solution and error:

$$\begin{aligned} u_m^{(1)} &= \tilde{u}_m + C_m h_1^{\alpha}, \\ u_m^{(2)} &= \tilde{u}_m + C_m h_2^{\alpha}. \end{aligned} \tag{1}$$

This equation enables to estimate the approximation error as $\Delta u_m^{(1)} \approx C_m h_1^{\alpha}$. To apply RE the convergence order α should be *a priori* known and the solutions should belong to the asymptotic range of the convergence (the upper order terms should be small and may be neglected). To ensure the sequence of solutions to belong the asymptotic range one should use several additional levels of mesh refinement that caused an additional computational cost. The traditional domain for the Richardson extrapolation corresponds to the elliptic and parabolic problems with smooth solutions. The behavior of Richardson extrapolation error estimates for simulations of solutions with jumps, such as shock and contact lines for fluid mechanics, is known to be problematic [4,5]. It is caused by the fact that for CFD problems of inviscid compressible fluid containing shock waves and contact discontinuities the error order is essentially spatially local and depends on the type of flow structure [3,4,11,12]. So, it is necessary to extend RE for the additional estimation of the local order of convergence that is performed by [3,5].

The pointwise results of numerical computation for three consequent meshes of different steps (to avoid the interpolation issue, the steps corresponds consequent doubling of the number of grid nodes: $h_q \sim (1/2)^{q-1}$, $q = 1,2,3$) may be presented as:

$$\begin{aligned} u_m^{(1)} &= \tilde{u}_m + C_m h_1^{\alpha_m}, \\ u_m^{(2)} &= \tilde{u}_m + C_m h_2^{\alpha_m}, \\ u_m^{(3)} &= \tilde{u}_m + C_m h_3^{\alpha_m}. \end{aligned} \tag{2}$$

This system (generalized Richardson extrapolation (GRE), [3]) may be resolved regarding $\tilde{u}_m$, C_m, α_m by several methods described by [3-5] if C_m is independent

ICCS Camera Ready Version 2021
To cite this paper please use the final published version:
DOI: 10.1007/978-3-030-77980-1_42

on h and higher order terms may be neglected, that is, the solution is in the asymptotic range. This approach requires the use of several sequentially refined grids. The number of such grids can increase if the results for the coarse grid fall outside the asymptotic range. Unfortunately, in the contrast to the standard RE, the estimation of α_m is the ill-posed problem [5] and requires a regularization in order to obtain the stable results. The approximation error on the rough grid in the frame of GRE may be estimated as

$$\Delta u_m^{(1)} \approx C_m h_1^{\alpha_m} . \quad (3)$$

It should be mentioned that the accuracy of RE (and GRE) for the error estimation remains unresolved quantitatively that excludes estimates by computable inequalities of the form $\left|\Delta u_m^{(1)}\right| \leq C$. So, the Richardson extrapolation provides the pointwise approximation for the error field at the cost of the extremely high computational burden, requires a regularization (in its generalized form) and does not provide the mathematically rigorous estimates in the form of the inequality.

3 The relation of approximation error and the distances between numerical solutions

Let's consider the approximation error estimation using the distances between numerical solutions treated using the Inverse problem in accordance with [7]. We analyze an ensemble of numerical solutions $u_m^{(i)}$ ($i = 1 \ldots n$), obtained by n different numerical algorithms (different solvers) on the same grid. Herein, we apply certain vectorization, so m is the grid point number ($m = 1,\ldots,L$). We note the projection of the exact solution $\tilde{u}$ onto the grid as $\tilde{u}_{h,m}$ and the approximation error for i-th solution as $\Delta u_m^{(i)}$ $\left(u_m^{(i)} = \tilde{u}_m + \Delta u_m^{(i)}\right)$. Since the differences of numerical solutions $d_{ij,m} = u_m^{(i)} - u_m^{(j)} = \tilde{u}_{h,m} + \Delta u_m^{(i)} - \tilde{u}_{h,m} - \Delta u_m^{(j)} = \Delta u_m^{(i)} - \Delta u_m^{(j)}$ are equal to the differences of approximation errors one may get $N = n \cdot (n-1)/2$ independent equations relating unknown approximation errors and computable differences of numerical solutions

$$D_{ij} \Delta u_m^{(j)} = f_{i,m} . \quad (4)$$

Herein, D_{ij} is a rectangular $N \times n$ matrix, $f_{i,m}$ is a vectorized form of the ences $d_{ij,m}$, the summation over a repeating index is implied.

Formally, the approximation error may be expressed as

$$\Delta u_m^{(j)} = (D_{ij})^{-1} f_{i,m} . \quad (5)$$

In the considered case ($n = 4$) the equation (4) has the form

ICCS Camera Ready Version 2021
To cite this paper please use the final published version:
DOI: 10.1007/978-3-030-77980-1_42

$$\begin{pmatrix} 1 & -1 & 0 & 0 \\ 1 & 0 & -1 & 0 \\ 1 & 0 & 0 & -1 \\ 0 & 1 & -1 & 0 \\ 0 & 1 & 0 & -1 \\ 0 & 0 & 1 & -1 \end{pmatrix} \begin{pmatrix} \Delta u_m^{(1)} \\ \Delta u_m^{(2)} \\ \Delta u_m^{(3)} \\ \Delta u_m^{(4)} \end{pmatrix} = \begin{pmatrix} f_{1,m} \\ f_{2,m} \\ f_{3,m} \\ f_{4,m} \\ f_{5,m} \\ f_{6,m} \end{pmatrix} = \begin{pmatrix} u_m^{(1)} - u_m^{(2)} \\ u_m^{(1)} - u_m^{(3)} \\ u_m^{(1)} - u_m^{(4)} \\ u_m^{(2)} - u_m^{(3)} \\ u_m^{(2)} - u_m^{(4)} \\ u_m^{(3)} - u_m^{(4)} \end{pmatrix}. \quad (6)$$

At the first glance the system is overdetermined. However, the solution of system (4) is invariant relatively a simultaneous shift transformation of all terms $u_m^{(j)} = \tilde{u}_m^{(j)} + b$ (and corresponding errors $\Delta u_m^{(j)} = \Delta\tilde{u}_m^{(j)} + b$) for any $b \in (-\infty, \infty)$ due to the usage of the difference of solutions as the input data. For this reason, the problem of approximation error estimation from the difference of solutions is really underdetermined and therefore ill-posed. We solve the system of equations (6) by the method considered in following section.

4 The estimation of approximation error using regularized Inverse Problem

In general, a regularization ([8,9]) is necessary in order to obtain the steady and bounded solution of the ill-posed problems. Herein we apply the zero order Tikhonov regularization in order to obtain solutions with the minimum shift error $|b|$. The minimal L_2 norm of $\Delta u^{(j)}$ restricts the absolute value of b, since:

$$\min_{b_m}(\delta(b_m)) = \min_{b_m} \sum_{j}^{n} (\Delta u_m^{(j)})^2/2 = \min_{b_m} \sum_{j}^{n} (\Delta\tilde{u}_m^{(j)} + b_m)^2/2. \quad (7)$$

This expression is used as the regularizing term in variational statement of the Inverse Problem.

One may see that

$$\Delta\delta(b_m) = \sum_{j}^{n} (\Delta\tilde{u}_m^{(j)} + b_m)\Delta b_m, \quad (8)$$

and the minimum occurs at b_m that equals the mean error (with the opposite sign):

$$b_m = -\frac{1}{n}\sum_{j}^{n} \Delta\tilde{u}_m^{(j)} = -\Delta\bar{u}_m. \quad (9)$$

So, the expression (7) may be treated as the minimum of the deviation of the exact error from the mean $\Delta u^{(j)} = \Delta\tilde{u}^{(j)} - \Delta\bar{u}$ (the exact error dispersion). The minimality

ICCS Camera Ready Version 2021
To cite this paper please use the final published version:
DOI: 10.1007/978-3-030-77980-1_42

of δ ensures the boundedness of the shift error b_m. Thus, the accuracy of the error $\Delta u^{(j)}$ estimation in considered approach is restricted by the mean error value.

We pose the Inverse Problem for $\Delta u^{(j)}$ estimation in the variational statement [9] that implies the minimization of the following functional:

$$\varepsilon_m(\Delta\vec{u}) = 1/2(D_{ij}\Delta u_m^{(j)} - f_{i,m})\cdot(D_{ik}\Delta u_m^{(k)} - f_{i,m}) + \alpha/2(\Delta u_m^{(j)} E_{jk}\Delta u_m^{(k)}) . \quad (10)$$

The first term of (10) is the discrepancy of the predictions and observations, the second term is the zero order Tikhonov regularization (α is the regularization parameter, E_{jk} is the unite matrix). We apply the gradient based (steepest descent) iterations (k is the number of the iteration) for the minimization of the functional:

$$\Delta u_m^{(j),k+1} = \Delta u_m^{(j),k} - \tau\nabla\varepsilon_m . \quad (11)$$

The gradient is obtained in the present work by the direct numerical differentiation, the iterations terminate at certain small value of the functional $\varepsilon \le \varepsilon_*$ ($\varepsilon_* = 10^{-8}$ was used). The obtained solution depends on the choice of the regularization parameter α. Without regularization ($\alpha = 0$) $|\Delta u^{(j)}(\alpha)|$ is not bounded and is not acceptable for this reason. The limit $\alpha \to \infty$ is not acceptable also, since $|\Delta u^{(j)}(\alpha)| \to 0$. A range of the regularization parameter α exists where the weak dependence of the solution on α is manifested. In this range, the solution $\Delta u^{(j)}(\alpha)$ is close to the exact one $\Delta\tilde{u}^{(j)}$ and is considered as the regularized solution [8]. By the rearranging Eq. (10) one may obtain

$$\varepsilon_m^{(1)}(\Delta\vec{u}) = 1/2(\Delta u_m^{(j)} E_{jk}\Delta u_m^{(k)}) + 1/(2\alpha)(D_{ij}\Delta u_m^{(j)} - f_{i,m})\cdot(D_{ik}\Delta u_m^{(k)} - f_{i,m}) \quad (12)$$

and

$$\varepsilon_m^{(1)}(\Delta\vec{u}) = \varepsilon_m(\Delta\vec{u})/\alpha . \quad (13)$$

This expression enables the estimation of the mean local error in the form of inequality:

$$\sum_k \left\|\Delta u_m^{(k)}\right\|^2 \le 2\varepsilon_m^{(1)} . \quad (14)$$

The corresponding estimation of the global error norm has the appearance

$$\sum_k \left\|\Delta u^{(k)}\right\|^2 \le 2/M \cdot \sum_{m=1}^{M} \varepsilon_m^{(1)} . \quad (15)$$

So, in contrast to the Richardson extrapolation, the Inverse Problem based approach enables the estimation of the averaged error in the form of strict inequalities.

ICCS Camera Ready Version 2021
To cite this paper please use the final published version:
DOI: 10.1007/978-3-030-77980-1_42

5 The test problem

The estimation of the approximation error for the problems containing discontinuities is a challenging task. In CFD problems the errors arising at shock waves and contact discontinuities are of the significant magnitude, demonstrate the oscillating behavior and are specified by nonstandard order of the convergence. For this reason our attention in the present paper is focused on the errors engendered by the shock waves. The similar topics arising at the contact discontinuities and the shock interferences are reserved for the future works. The test problem is governed by the two dimensional compressible Euler equations describing a shock wave. The following flowfield parameters: density, velocity components along x and y axes, pressure ($\{\rho, v_x, v_y, p\}$) and the Mach number (M) are used in the analysis. We estimate the approximation error by minimizing the functional (7) using Expression (11) for parameters $u_m^{(i)}$ that correspond the flowfield variables $\{\rho, v_x, v_y, p\}$ at every grid point. The flowfield around a plate at the angle of attack $\alpha = 6°$ and $\alpha = 20°$ in the uniform supersonic flow ($M = 2$ and $M = 4$) of ideal gas is analyzed. The approximation error is estimated using generalized Richardson extrapolation [3,5] and the Inverse problem based statement. The results are compared with the exact error obtained by the subtraction of the numerical solution and the projection of the analytic solution on the computational grid. At $\alpha = 6°$ and $M = 2$ we obtain a relatively weak shock wave, while at $\alpha = 20°$ and $M = 4$ the shock wave is strong. On the left boundary ("*inlet*") and on the upper boundary *("top")*, the inflow parameters are set for Mach number $M = 2$, $M = 4$ an corresponding angles. On the right boundary ("*outlet*") the zero gradient condition for the gas dynamic functions is specified. On the plate surface, the condition of zero normal gradient is posed for the pressure and the temperature, and the condition "*slip*" is posed for the speed, corresponding to the non-penetration. The parameters of the OpenFOAM package are the same as in [7].

6 OpenFOAM solvers

The solvers from the OpenFOAM software package [13] that were used are the following:

- *rhoCentralFoam* (marked as rCF), which is based on a central-upwind scheme [14,15].
- *sonicFoam* (sF), which is based on the PISO algorithm [16].
- *pisoCentralFoam* (pCF) [17], which combines the Kurganov-Tadmor scheme [14] and the PISO algorithm [16].
- *QGDFoam* (QGDF), which implements the quasi-gas dynamic equations [18].

These solvers are of the second approximation order, while they are based on the algorithms of the quite different ideas and inner structure.

ICCS Camera Ready Version 2021
To cite this paper please use the final published version:
DOI: 10.1007/978-3-030-77980-1_42

7 Numerical results

The exact errors are obtained by the comparison of the numerical solution with the analytic one for the shock wave (Rankine-Hugoniot relations). The relative exact errors in L_1 and L_2 norms are presented in Tables 1-6 for $\alpha = 20°$, $M = 4$ and three grids (20000, 80000 and 320000 nodes). For QGDF code the coefficient $\beta = 0.1$ is used that controls the artificial viscosity.

Table 1. The relative errors in L_1 norm (M = 4, α = 20°, 20000 nodes).

	rCF	pCF	sF	QGDF
M	0.001295	0.001489	0.002267	0.01155
p	0.010745	0.011226	0.025567	0.018022
ρ	0.005817	0.006573	0.015622	0.008541

Table 2. The relative errors in L_1 norm (M = 4, α = 20°, 80000 nodes).

	rCF	pCF	sF	QGDF
M	0.000701	0.000816	0.001205	0.000611
p	0.005512	0.005964	0.013733	0.009629
ρ	0.003086	0.003601	0.008663	0.004549

Table 3. The relative errors in L_1 norm (M = 4, α = 20°, 320000 nodes).

	rCF	pCF	sF	QGDF
M	0.000381	0.000439	0.000678	0.000439
p	0.002944	0.003217	0.007621	0.003217
ρ	0.001654	0.001938	0.005043	0.001938

Table 4. The relative errors in L_2 norm (M = 4, α = 20°, 20000 nodes).

	rCF	pCF	sF	QGDF
Ma	0.013951	0.015138	0.013520	0.009920
p	0.080503	0.079493	0.143794	0.098895
ρ	0.047797	0.047157	0.092308	0.055613

Table 5. The relative errors in L_2 norm (M = 4, α = 20°, 80000 nodes)

	rCF	pCF	sF	QGDF
M	0.010127	0.011202	0.009191	0.007125
p	0.055094	0.056591	0.104672	0.070171
ρ	0.033143	0.033612	0.066215	0.039410

ICCS Camera Ready Version 2021
To cite this paper please use the final published version:
DOI: 10.1007/978-3-030-77980-1_42

Table 6. The relative errors in L_2 norm (M = 4, α = 20°, 320000 nodes)

	rCF	pCF	sF	QGDF
M	0.007527	0.008263	0.006610	0.008263
p	0.039382	0.040675	0.081605	0.040675
ρ	0.024024	0.024262	0.051199	0.024262

Tables 1-6 demonstrate the order of convergence about 1.0 in L_1 norm and about 0.5 in L_2 that is far from the nominal (second) order of considered algorithms and corresponds results by [3,4,11,12].

We estimate the approximation error using the generalized Richardson extrapolation [3,5] on three consequent grids containing 20000, 80000 and 320000 nodes (with doubling number of nodes along both directions at every refinement).

In the inverse problem statement, we minimize the functional (7) for each flow parameter from the set $\{\rho, v_x, v_y, p\}$ separately at every grid point.

The Figs. 1-5 present the pieces of vectorized grid function of density error obtained by the Inverse Problem in comparison with the results of the generalized Richardson extrapolation and the exact error. The index along abscissa axis $i = N_x(k_x - 1) + m_y$ is defined by indexes along $X(k_x)$ and $Y(m_y)$. The periodical jump of solution variables corresponds to the transition through the shock wave. One may see that the error at the shock wave is under resolved by both (RE and IP) methods. This behavior is expected since the error at a shock tends to be singular at the mesh refinement.

The impact of the shock wave intensity on the quality of the error estimation may be observed from Figs 1 and 2 that demonstrate the dependence of both the IP-based and GRE estimation quality on the strength of the shock wave (for $M = 2$ and $M = 4$ correspondingly). The Fig. 1 presents the piece of vectorized grid function of density error (computed by rCF) for $\alpha = 6°$, $M = 2$. The Fig. 2 presents the piece of vectorized grid function of density error (computed by rCF) for $\alpha = 20°$, $M = 4$. For the small approximation error (small Mach number and deflection angle, Fig. 1) the generalized Richardson extrapolation outperforms the Inverse problem based results despite some instability past shock wave. These results are expectable, since the Richardson extrapolation is known to well behave for the rather regular solutions (weak shock waves in our case). For the relatively great approximation errors the IP-based results are rather smoothed and shifted in comparison with the exact error. This is caused by the using the set of solutions having slightly shifted position of the shock waves. Nevertheless the total quality of the IP-based error estimate improves and may compete with the results obtained by GRE (which suffer from instabilities).

ICCS Camera Ready Version 2021
To cite this paper please use the final published version:
DOI: 10.1007/978-3-030-77980-1_42

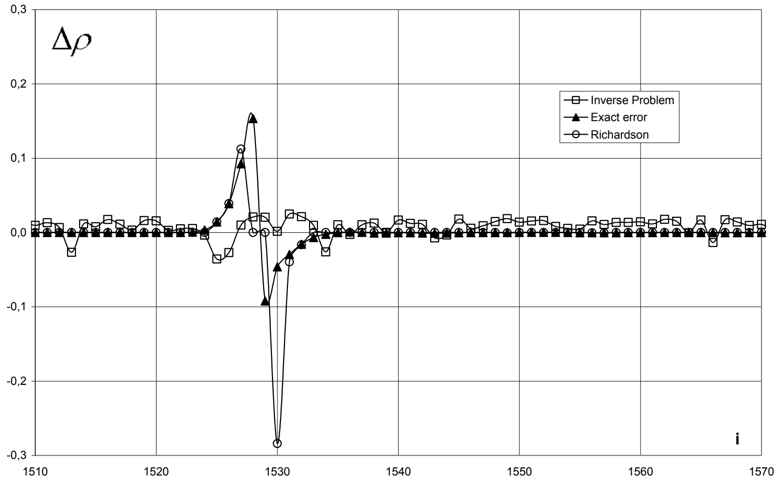

Fig. 1. The comparison of the vectorized density error (rCF), estimated by the Inverse Problem and GRE with the exact error for M=2.

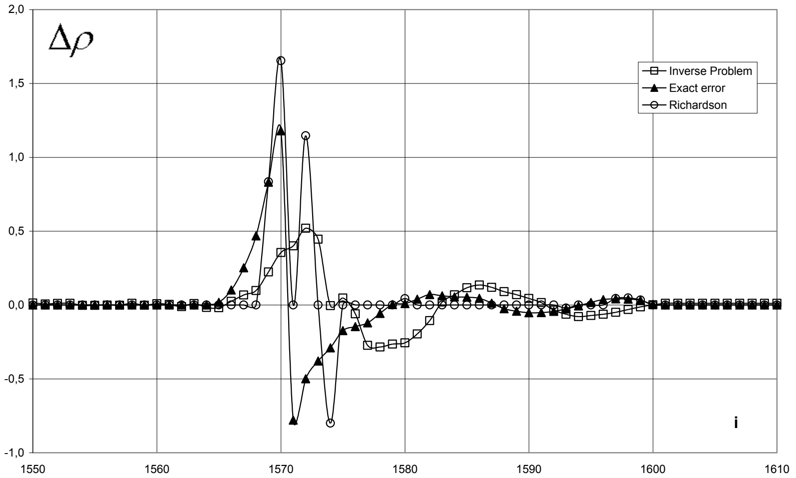

Fig. 2. The comparison of the vectorized density error (rCF), estimated by the Inverse Problem and GRE with the exact error for M=4.

The Figs. 3-5 provide the density errors ($\alpha = 20°$, $M = 4$) for pCF, QGDF, and sF correspondingly.

ICCS Camera Ready Version 2021
To cite this paper please use the final published version:
DOI: 10.1007/978-3-030-77980-1_42

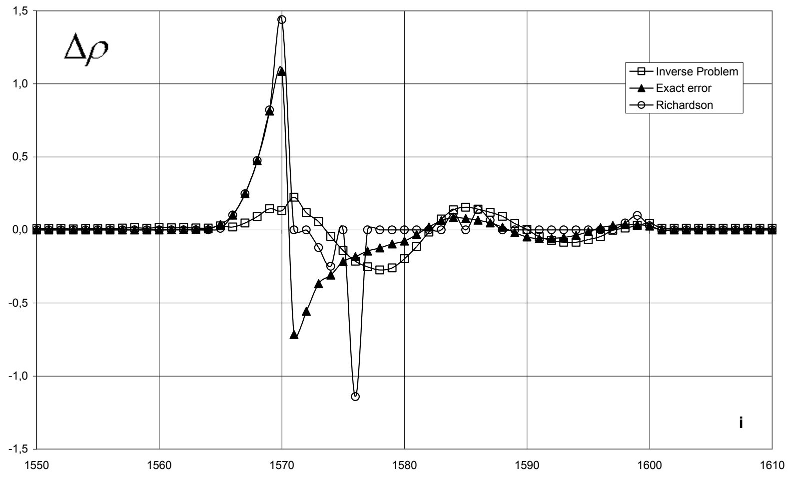

Fig. 3. The comparison of the vectorized density error (pCF), estimated by the Inverse Problem and GRE with the exact error for M=4.

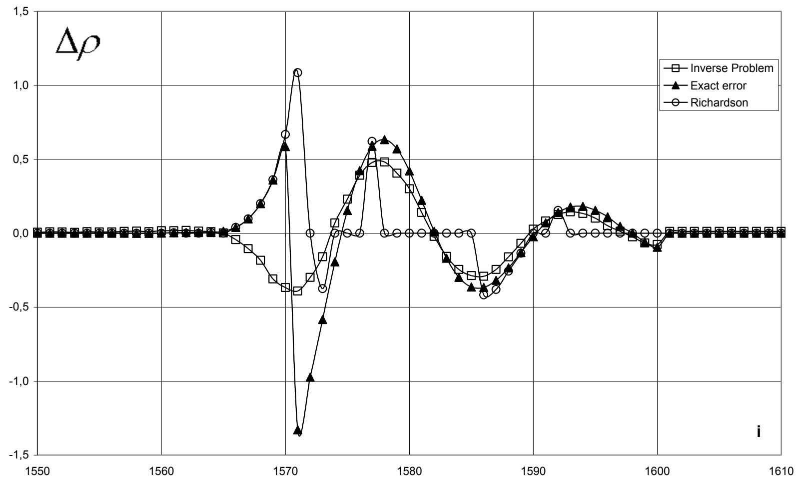

Fig. 4. The comparison of the vectorized density error (QGD), estimated by the Inverse Problem and GRE with the exact error for M=4.

ICCS Camera Ready Version 2021
To cite this paper please use the final published version:
DOI: 10.1007/978-3-030-77980-1_42

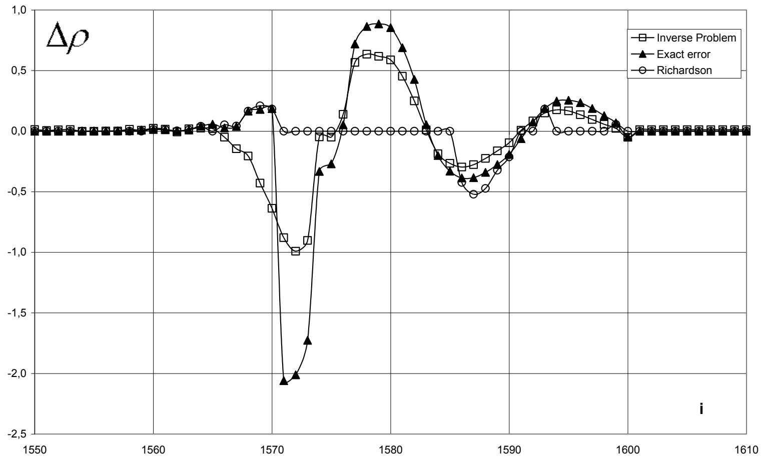

Fig. 5. The comparison of the vectorized density error (sF), estimated by the Inverse Problem and GRE with the exact error for M=4.

The results significantly depend on the choice of the solver. On the above numerical tests the sF solver provides most error over all set of codes (see Tables 1-6).

The quality of *a posteriori* error estimate may be described by the effectivity index [19] that equals the relation of the estimated error norm to the exact error norm:

$$I_{eff,k} = \left\|\Delta\vec{\rho}^{(k)}\right\|_{L_2} / \left\|\Delta\vec{\tilde{\rho}}^{(k)}\right\|_{L_2} \tag{16}$$

The vectors $\Delta\vec{\rho}^{(k)}, \Delta\vec{\tilde{\rho}}^{(k)} \in R^M$ (M is the number of grid nodes) in this relation denote the grid functions. Thus, the norms, herein, imply averaging of pointwise errors over the total flowfield. To provide the reliability of the error estimation, this index should be greater the unit. On the other hand, the estimation should be not too pessimistic, so the value of the effectivity index should be not too great. According [19], the range $1 \le I_{eff} \le 3$ is acceptable for the finite elements in the domain of elliptic equations. However, for the present discontinuous solutions these values are problem dependent. The upper bound may by corrected using the tolerance of the valuable functionals and the Cauchy–Bunyakovsky–Schwarz inequality [6]. The down boundary may be corrected using certain safety coefficient. The corresponding values of the effectivity index are provided in the Tables 7 and 8 for IP-based statement and the Richardson extrapolation.

Table 7. Effectivity indexes of error estimation (α = 6°, M = 2).

	I_{eff}^{rCF}	I_{eff}^{pCF}	I_{eff}^{sF}	I_{eff}^{QGDF}
IP	0.316	0.315	0.631	0.385
Richardson	1.151	1.253	3.366	0.965

ICCS Camera Ready Version 2021
To cite this paper please use the final published version:
DOI: 10.1007/978-3-030-77980-1_42

Table 8. Effectivity indexes of error estimation (α = 20°, M = 4).

	I_{eff}^{rCF}	I_{eff}^{pCF}	I_{eff}^{sF}	I_{eff}^{QGDF}
IP	0.316	0.315	0.631	0.385
Richardson	1.151	1.253	3.366	0.965

Tables 7 and 8 present the effectivity index for $M = 2$ and $M = 4$. One may see that the reliability of the Richardson extrapolation decreases as the intensity of the shock waves increases (Mach number and flow deflection angle rise). On contrary, the reliability of the IP-based estimated increases. In general, from the standpoint of the global error estimation the GRE provides more reliable results.

Especially important is the question of comparing the computational costs for the GRE and IP methods for a given test problem. Since the Richardson extrapolation requires a sequence of grids (in this case 3), with doubling the number of grid nodes, it turns out to be very expensive both in terms of computational complexity and memory costs. If we apply the Inverse Problem, we need only a few numerical solutions obtained by different methods on the same grid. If we assume that the methods do not differ much in computational and memory costs, then the memory costs required by the Richardson extrapolation are 5.25 times greater than the memory costs required by the IP approach. The calculation time ratio is about 18. Additional acceleration of computations in the IP approach can be achieved by constructing a generalized computational experiment [22]. The construction of a generalized computational experiment is based on the simultaneous solution using parallel computations in a multitasking mode of a basic problem with different input parameters, obtaining results in the form of multidimensional data volumes and their visual analysis. Using a generalized computational experiment, we can apply the IP approach, calculating in parallel the problem for each solver on its own node of the computational cluster in a multitasking mode, which provides additional acceleration of computations.

8 Discussion

In the paper [7] the Inverse Problem based approach was used for the supersonic axisymmetric flows around cones. The comparison with the etalon (high precision solution by [10]) was presented. In [20] the flow modes obtained by the crossing shocks (Edney-I and Edney-VI patterns by [21]) are analyzed. Herein, the comparison for the flat flow is performed for the Inverse Problem based errors, exact error (obtained by the comparison with the analytic solutions) and the results of the Richardson approximation. Formally, the Inverse Problem based approach is less accurate if compared with the Richardson extrapolation due to the presence of the unremovable error, proportional to the mean error over the ensemble of solutions. However, this statement is valid only for the highly smooth solutions. For the above considered problems with shock waves the generalized Richardson extrapolation should be used that is the highly unstable, that deteriorates the results. In most cases, the GRE demonstrates highly nonsmooth solutions that may approximate the part of the exact error (usually, before

ICCS Camera Ready Version 2021
To cite this paper please use the final published version:
DOI: 10.1007/978-3-030-77980-1_42

the shock wave) with a relatively high resolution, while another part of the exact error (past the shock wave) is poorly approximated. The comparison of the results obtained by GRE and IP with the exact error demonstrates the high smoothing properties of the pointwise IP error estimation and the visible shift of the error location. Since the IP-based error estimate are polluted by the mean error over the ensemble (9), the best results are obtained for the less accurate solutions (herein, for sF, see Fig. 5).

In general, numerical tests demonstrate the accuracy of the error estimates obtained using generalized Richardson extrapolation to be superior in the comparison with the Inverse Problem based results for the weak shocks and comparable for the strong shocks. In contrast to the generalized Richardson extrapolation, the considered IP-based postprocessor is much more computationally inexpensive, since it uses only single grid computations. Additionally, it possesses some natural parallelism, since different solvers may be independently computed by different nodes of the cluster, which fits into the concept of constructing a generalized computational experiment [22].

9 Conclusion

The numerical tests demonstrate the feasibility for the estimation of the point-wise approximation error via the Inverse Problem treating of the ensemble of numerical solutions obtained using the four solvers from the OpenFOAM software package for the two-dimensional inviscid flow pattern engendered by the oblique shock wave. The Inverse Problem based estimation of the point-wise approximation error using the differences of numerical solutions as the input data provides the accuracy comparable with the generalized Richardson extrapolation, however, it is much more computationally inexpensive.

Acknowledgments

This work was supported by grant of RSF № 18-11-00215.

References

1. Guide for the Verification and Validation of Computational Fluid Dynamics Simulations, American Institute of Aeronautics and Astronautics, AIAA-G-077-1998, 1998.
2. Standard for Verification and Validation in Computational Fluid Dynamics and Heat Transfer, ASME V&V 20-2009, 2009.
3. Roy, Ch. J.: Grid Convergence Error Analysis for Mixed-Order Numerical Schemes. AIAA Journal 41(4), 595–604 (2003). https://doi.org/10.2514/2.2013
4. Banks, J. W., Aslam, T. D.: Richardson Extrapolation for Linearly Degenerate Discontinuities. Journal of Scientific Computing 57, 1–15 (2013). https://doi.org/10.1007/s10915-013-9693-0
5. Alekseev, A.K., Bondarev, A.E.: On some features of Richardson extrapolation for compressible inviscid flows. Mathematica Montisnigri XL, 42–54 (2017)

ICCS Camera Ready Version 2021
To cite this paper please use the final published version:
DOI: 10.1007/978-3-030-77980-1_42

6. Alekseev A.K., Bondarev A. E., Kuvshinnikov A. E.: On uncertainty quantification via the ensemble of independent numerical solutions. Journal of Computational Science. 42, 10114 (2020). https://doi.org/10.1016/j.jocs.2020.101114
7. Alekseev A.K., Bondarev A. E., Kuvshinnikov A. E.: A posteriori error estimation via differences of numerical solutions, in V. V. Krzhizhanovskaya et al. (Eds.): ICCS 2020. Lecture Notes in Computer Science (LNCS), vol. 12143, pp. 508–519. Springer, Cham (2020). https://doi.org/10.1007/978-3-030-50436-6_37
8. Tikhonov, A.N., Arsenin, V.Y.: Solutions of Ill-Posed Problems. Winston and Sons, Washington DC (1977).
9. Alifanov, O.M., Artyukhin, E.A., Rumyantsev S.V.: Extreme Methods for Solving Ill-Posed Problems with Applications to Inverse Heat Transfer Problems. Begell House (1995).
10. Babenko, K.I., Voskresenskii, G.P., Lyubimov, A.N., Rusanov, V.V.: Three-dimensional ideal gas flow past smooth bodies. Nauka, Moscow (1964). (In Russian)
11. Carpenter, M. H., Casper, J.H.: Accuracy of Shock Capturing in Two Spatial Dimensions. AIAA J. 37(9), 1072–1079 (1999). https://doi.org/10.2514/2.835
12. Godunov, S.K., Manuzina, Yu.D., Nazareva, M.A.: Experimental analysis of convergence of the numerical solution to a generalized solution in fluid dynamics. Computational Mathematics and Mathematical Physics 51, 88–95 (2011). https://doi.org/10.1134/S0965542511010088
13. OpenFOAM, http://www.openfoam.org. Accessed 25 Jan 2021
14. Kurganov, A., Tadmor, E.: New high-resolution central schemes for nonlinear conservation laws and convection-diffusion equations. J. Comput. Phys. 160(1), 241–282 (2000). https://doi.org/10.1006/jcph.2000.6459
15. Greenshields, C., Wellerr, H., Gasparini, L., Reese, J.: Implementation of semi-discrete, non-staggered central schemes in a colocated, polyhedral, finite volume framework, for high-speed viscous flows. Int. J. Numer. Meth. Fluids 63(1), 1–21 (2010). https://doi.org/10.1002/fld.2069
16. Issa, R.: Solution of the implicit discretized fluid flow equations by operator splitting. J. Comput. Phys. 62(1), 40–65 (1986). https://doi.org/10.1016/0021-9991(86)90099-9
17. Kraposhin, M., Bovtrikova, A., Strijhak, S.: Adaptation of Kurganov-Tadmor numerical scheme for applying in combination with the PISO method in numerical simulation of flows in a wide range of Mach numbers. Procedia Computer Science 66, 43–52 (2015). https://doi.org/10.1016/j.procs.2015.11.007
18. Kraposhin, M.V., Smirnova, E.V., Elizarova, T.G., Istomina, M.A.: Development of a new OpenFOAM solver using regularized gas dynamic equations. Computers & Fluids 166, 163–175 (2018). https://doi.org/10.1016/j.compfluid.2018.02.010
19. Repin, S.I.: A posteriori estimates for partial differential equations. Vol. 4. Walter de Gruyter (2008). https://doi.org/10.1515/9783110203042
20. Alekseev A., Bondarev A.: The Estimation of Approximation Error using the Inverse Problem and the Set of Numerical Solutions, arXiv:2101.00381v1 (2021)
21. Edney, B.: Effects of Shock Impingement on the Heat Transfer around Blunt Bodies. AIAA J. 6(1), 15–21 (1968). https://doi.org/10.2514/3.4435
22. Bondarev A.E.: On the Construction of the Generalized Numerical Experiment in Fluid Dynamics. Mathematica Montisnigri XLII, 52–64 (2018).

ICCS Camera Ready Version 2021
To cite this paper please use the final published version:
DOI: 10.1007/978-3-030-77980-1_42